

# Microstructural, mechanical and dry sliding wear properties of the MgO reinforced aluminium matrix composites produced by vacuum infiltration

O. Bican\*

*Department of Materials and Metallurgy Engineering, Kirikkale University, 71450, Kirikkale, Turkey*

Received 15 February 2012, received in revised form 24 March 2013, accepted 25 October 2013

## Abstract

Dry sliding wear properties of MgO (10–40 vol.%) reinforced aluminium matrix composites produced by vacuum infiltration method were investigated using a pin-on-disc test machine after examining their microstructural and mechanical properties. The hardness of the composites increased continuously with increasing MgO content and the highest hardness (71 HB) was obtained for Al-40vol.%MgO. The highest tensile strength (139 MPa) and the lowest porosity (1.3 %) were obtained for Al-20vol.%MgO composite. It was observed that the wear volume of the composites increased with increasing load and sliding speed. Wear resistance of the composites tested was observed to be strongly dependent on their tensile strength and porosity rather than their hardness. Although adhesion and abrasion took place during the wear of tested composites, smearing appeared to be the most effective wear mechanism for the composites containing up to 20 vol.% MgO, while abrasive wear dominated for the Al-30vol.%MgO and Al-40vol.% MgO composites.

**Key words:** vacuum infiltration, mechanical properties, MgO, aluminium matrix composites, wear

## 1. Introduction

Metal matrix composites are of a considerable interest over the last three decades [1–4]. Ceramic reinforcements (SiC, TiC, B<sub>4</sub>C, etc.) can improve the hardness, strength, fatigue and wear properties compared to traditional engineering materials [5–9]. However, the use of MMCs is hindered by their relatively poor fracture properties and brittleness [10]. To prevail over these disadvantages, aluminium based metal matrix composites are developed with different reinforcements [11–13]. Aluminium based MMCs can be produced by different methods such as powder metallurgy, in situ processes and infiltration methods [14–16]. Infiltration method: a molten metal matrix is incorporated into a solid porous ceramic reinforcement preform. An external driving force must be employed to force the infiltration of the liquid matrix into the reinforcement. A gas over pressure is applied to the free surface of the liquid metal (pressure infiltration)

or the reinforcement preform vented to either atmosphere (pressureless infiltration) or vacuum (vacuum infiltration).

MgO, which is a high temperature ceramic material, has been largely used as reinforcement in aluminium based MMCs [17]. MgO and Al have cubic structure and this raises the possibility of forming low energy interfaces between them at any orientation and gives better wetting characteristics [18]. In addition, the presence of O<sub>2</sub> gives rise to formation of MgAl<sub>2</sub>O<sub>4</sub> (magnesium aluminate) at the interface of MgO reinforcement and Al matrix [19, 20]. Recent works showed that MgO reinforced Al based MMCs could be easily produced by vacuum infiltration method. Parameters such as reinforcement powder size, volume ratio, vacuum value and molten metal temperature, which affect the manufacturability, were investigated by different researchers [17, 21]. However, dry sliding wear properties of MgO reinforced aluminium based MMCs produced by vacuum infiltration method have

\*Corresponding author: tel.: +90 318 3574242/1267; fax: +90 318 3572459; e-mail address: [bican@kku.edu.tr](mailto:bican@kku.edu.tr)

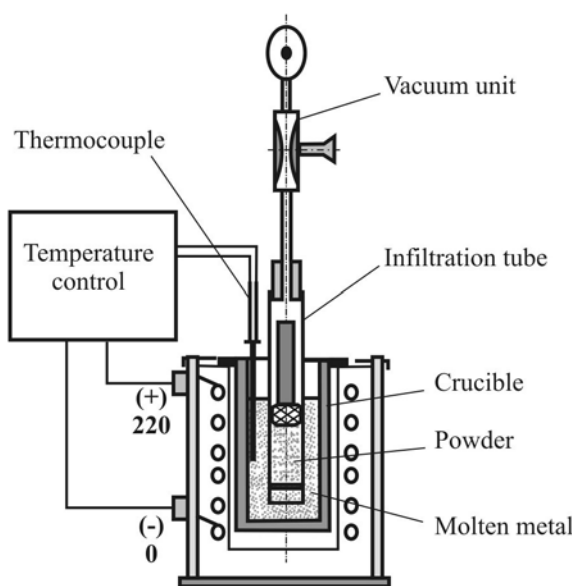


Fig. 1. Vacuum infiltration apparatus.

not been investigated under different test conditions. Therefore, the purpose of this study is to investigate the effects of the MgO content, pressure and sliding speed on the wear behaviour of the Al-based MMCs after determining their microstructural and mechanical properties.

## 2. Experimental procedure

### 2.1. Preparation of composites

Vacuum infiltration tests were carried out by using the prototype apparatus shown in Fig. 1. The system consists of a vacuum unit, an infiltration tube (quartz), and a crucible and temperature control system. Quartz tube has an outside diameter of 10 mm, a wall thickness of 1 mm and a length of 300 mm. Stainless steel filter and Al foil were placed at the bottom of the tube. Infiltration tests were performed with MgO powder filled to form 50 mm height. A filter, alumina blanket and a balance weight were placed on the powders to prevent the vacuuming of the powders. The molten metal temperature was kept 730 °C.  $500 \pm 5$  mm Hg vacuum was applied to the tube and the tube was dipped in liquid metal in normal atmosphere. The vacuum was kept under these conditions for 3 min. After 3 min of vacuuming, the tubes were taken out and cooled to the room temperature. The tubes were broken and composites were removed from the tubes. Commercially pure aluminium (99.7 %, Öz-ka Metal Ltd.) and MgO (0.6 % Fe, 1 % SiO<sub>2</sub> and 0.4 % CaO, TRS Ltd.) with  $d_{50} = 149$  µm were used as matrix and reinforcement phases,

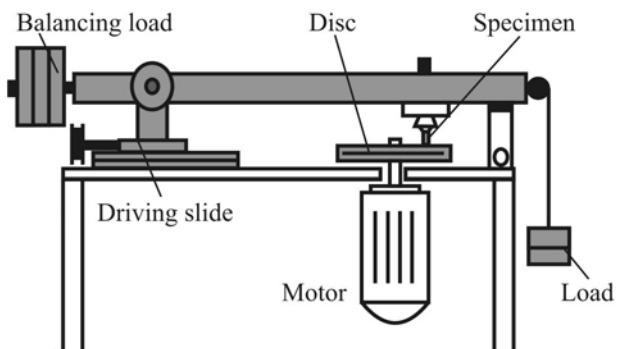


Fig. 2. Schematic diagram of the used wear test machine.

respectively. The particle size was determined using laser diffraction (Malvern, Model mastersizer Hydro 2000e) connected to a computer. Samples for microstructural examinations were prepared using standard metallographic techniques, etched with 3 % NaOH and examined by optical (Nikon MA-100) and scanning electron microscopy (Jeol JSM-6060 LV).

### 2.2. Physical and mechanical tests

The density of the composites was determined by water replacement method and porosity of the composites was measured using theoretical and experimental densities. Theoretical density values of the composites were obtained using the rule of mixture for composites. The Brinell hardness of the composites was measured using a load of 62.5 kg and 2.5 mm diameter steel ball as indenter. The tensile strength of the composites was measured using round specimens with a diameter of 6 mm and a gauge length of 30 mm at a strain rate of  $5.7 \times 10^{-3}$  s<sup>-1</sup>. All these physical and mechanical properties were determined by taking the average of at least three readings.

### 2.3. Wear tests

The wear tests were carried out using a prototype pin-on-disc test machine. A schematic diagram of the test machine is shown in Fig. 2. The machine consists of a disc, a pin (specimen) and its mounting system and a loading system. Specimens with 8 mm diameter and 30 mm length were prepared from Al-10vol.%MgO, Al-20vol.%MgO, Al-30vol.%MgO and Al-40vol.%MgO composites. Wear tests were performed at different loads (10–40 N) and sliding speeds ( $0.5\text{--}2.0$  m s<sup>-1</sup>) for a sliding distance of 40 m using 140 mesh (105 µm), 230 mesh (63 µm) and 320 mesh (44 µm) grain size Al<sub>2</sub>O<sub>3</sub> abrasive papers. The discs on the pin-on-disc machine were made of abrasive paper of different particle sizes. Each specimen was ultrasonically cleaned and weighed before wear tests using a balance with an accuracy of 0.01 mg. The

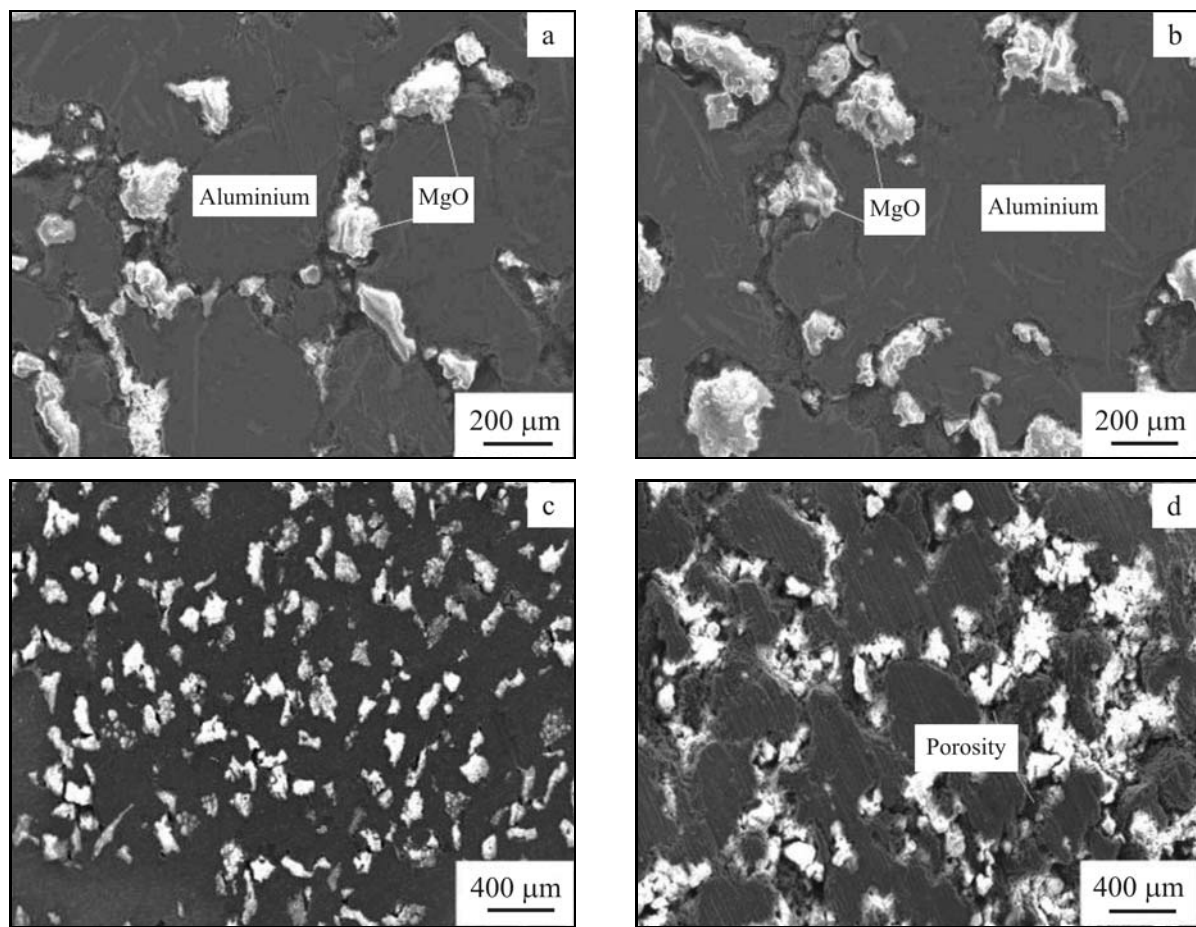


Fig. 3. Microstructure of the produced composites for different amounts of reinforcement phase: (a) Al-10vol.%MgO, (b) Al-20vol.%MgO, (c) Al-30vol.%MgO and (d) Al-40vol.%MgO.

Table 1. Density and porosity values of produced composites

Composite	Theoretical density ( $\text{g cm}^{-3}$ )	Experimental density ( $\text{g cm}^{-3}$ )	Porosity (%)	Uncertainty for porosity (%)
Al-10%MgO	2.72	2.65	2.51	0.6
Al-20%MgO	2.79	2.75	1.30	0.4
Al-30%MgO	2.86	2.62	8.20	1.1
Al-40%MgO	2.93	2.42	17.47	1.3

wear samples were removed after the test, cleaned in solvents (to eliminate the debris) and weighed to determine the mass loss. The measured values of mass loss for all the specimens tested were converted into volume loss using the measured density of the composites. The surface of the wear samples was examined using SEM.

### 3. Results

The SEM micrographs of the Al-MgO composites produced at different volume ratios by vacuum infilt-

ration method are shown in Figs. 3a–d. It can be seen from these figures that the microstructures of the composites consisted of Al matrix and MgO particles. It was observed that MgO particles showed a homogeneous distribution in the composites containing up to 20 % MgO. However, when the MgO content exceeded this level, MgO particles piled up in different locations.

The experimental and theoretical densities and porosity of the composites are given in Table 1. It was observed that the porosity of the composites decreased with increasing volume ratio up to 20 % MgO, above this level the trend reversed. The variation of the hardness, tensile strength and porosity of the MMCs as a

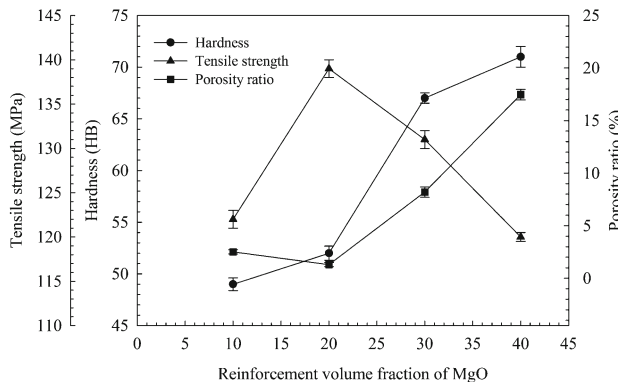


Fig. 4. Variation of hardness, tensile strength and porosity of the produced composites as a function of MgO contents.

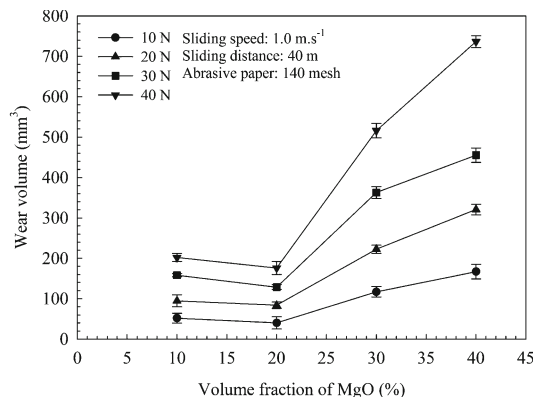


Fig. 5. Wear volume as a function of MgO volume fraction using 140 mesh abrasive paper.

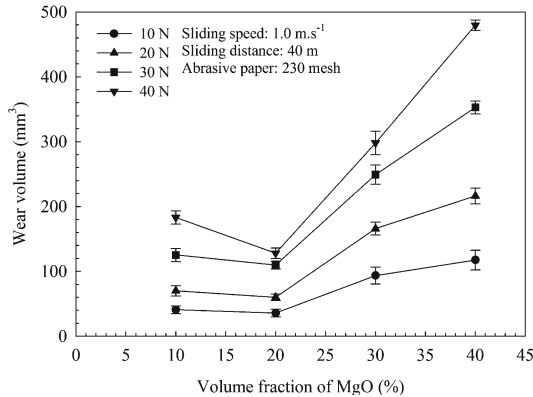


Fig. 6. Wear volume as a function of MgO volume fraction using 230 mesh abrasive paper.

function of MgO content are shown in Fig. 4. It can be seen that the hardness of the composites increased continuously with increasing MgO content. However, the tensile strength of the composites increased with increasing MgO content up to 20 %, above which the

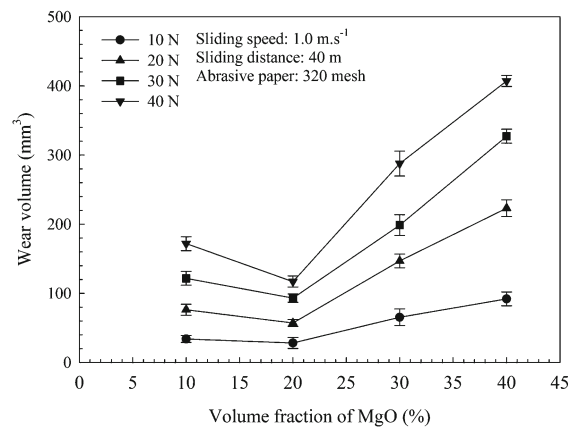


Fig. 7. Wear volume as a function of MgO volume fraction using 320 mesh abrasive paper.

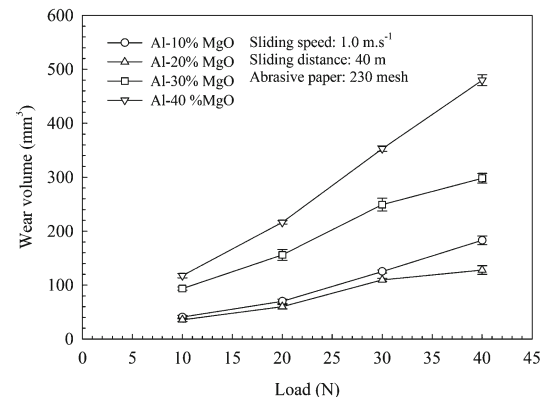


Fig. 8. Wear volume of the produced composites as a function of applied load.

tensile strength decreased with increasing MgO content.

The curves showing the change of wear volume at different loads and different mesh sizes as a function of volume fraction of MgO are given in Figs. 5–7. It can be seen that the wear volume of the composites decreased with increasing MgO content up to 20 %, above the trend reversed.

The changes of wear volume of the composites as a function of load and sliding speed are shown in Figs. 8, 9, respectively. It was observed that the wear volume of the composites increased with increasing load and sliding speed. The highest wear resistance was obtained for the Al-20%MgO composite.

Wear surfaces of the composites tested at a load of 20 N and a sliding speed of  $1 \text{ m s}^{-1}$  for a total sliding distance of 40 m are shown in Figs. 10a–d. The wear surfaces of the composites were characterized by smearing, scratches and grooves. As the MgO content increased in the composites, the scratches became larger and their number increased. On the other hand, the formation of grooves was observed on the wear sur-

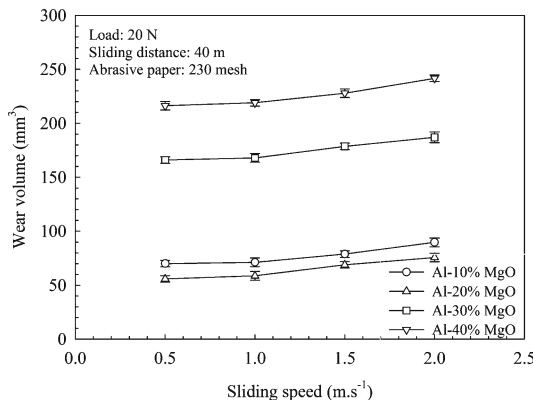


Fig. 9. Wear volume of the produced composites as a function of sliding speed.

face of the produced composites. It was observed that the number of grooves increased with increasing MgO content. The wear surface values of Al-20%MgO tested at different loads are shown in Figs. 11a–c. It was ob-

served that the number and width of the scratches and grooves on the wear surface of the composites increased with increasing load.

#### 4. Discussion

It was observed that the porosity of the composites decreased with increasing volume ratio up to 20 % MgO, above this level the trend reversed Figs. 3a–d. MgAl<sub>2</sub>O<sub>4</sub> (magnesium aluminate) may be formed in the interface of MgO reinforcement and Al matrix under the 20 vol. % MgO. It is known that formation of magnesium aluminate gives better wetting characteristics with Al and its alloys [19, 20].

MgO particles showed a homogeneous distribution in the composites containing up to 20 % MgO. However, when the MgO content exceeded this level, MgO particles piled up in different locations. This may be due to the sticking and collision of these particles in the liquid metal during vacuum infiltration process. It was observed that the hardness of the compos-

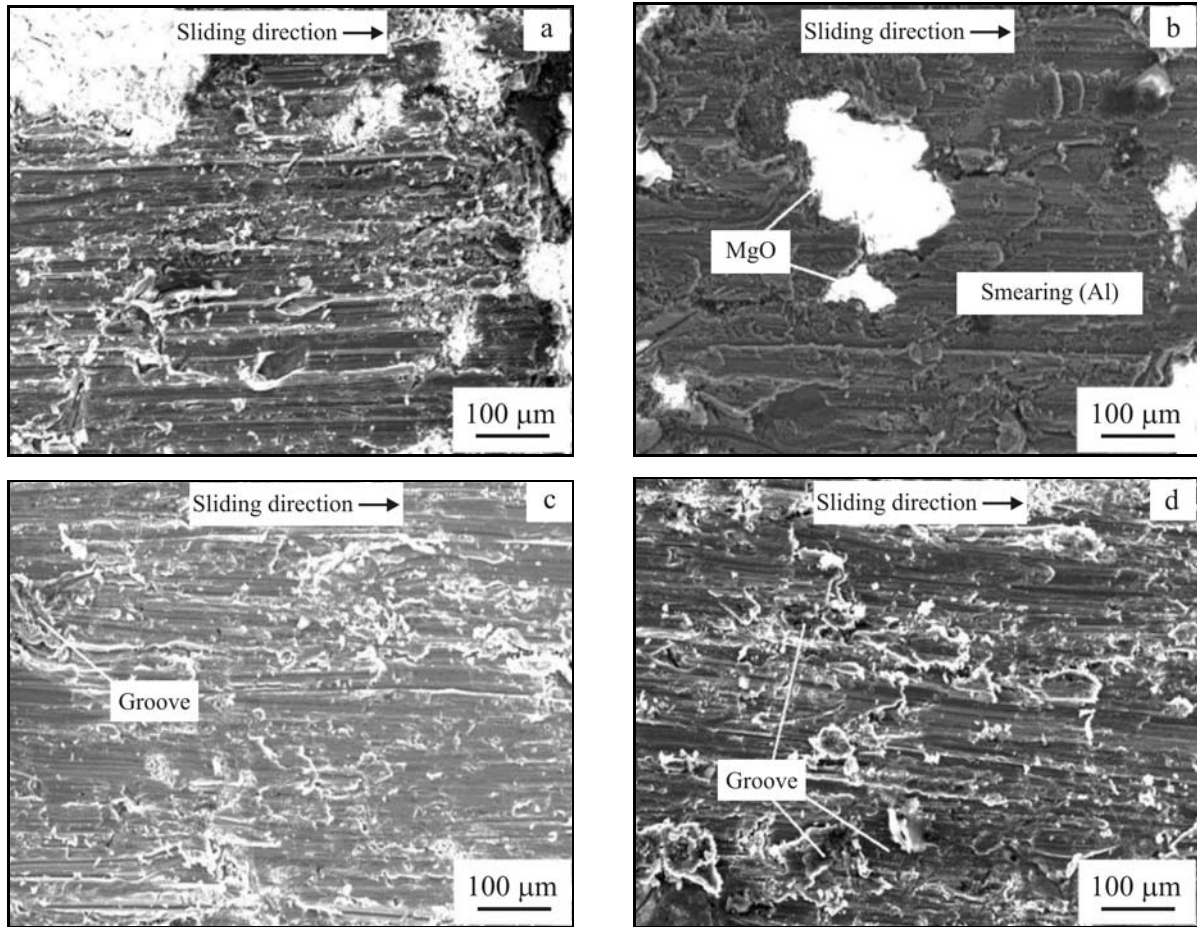


Fig. 10. Wear surfaces of (a) Al-10%MgO, (b) Al-20%MgO, (c) Al-30%MgO and (d) Al-40%MgO composites tested at a load of 20 N and a speed of 1.0 m s⁻¹ for a sliding distance of 40 m.

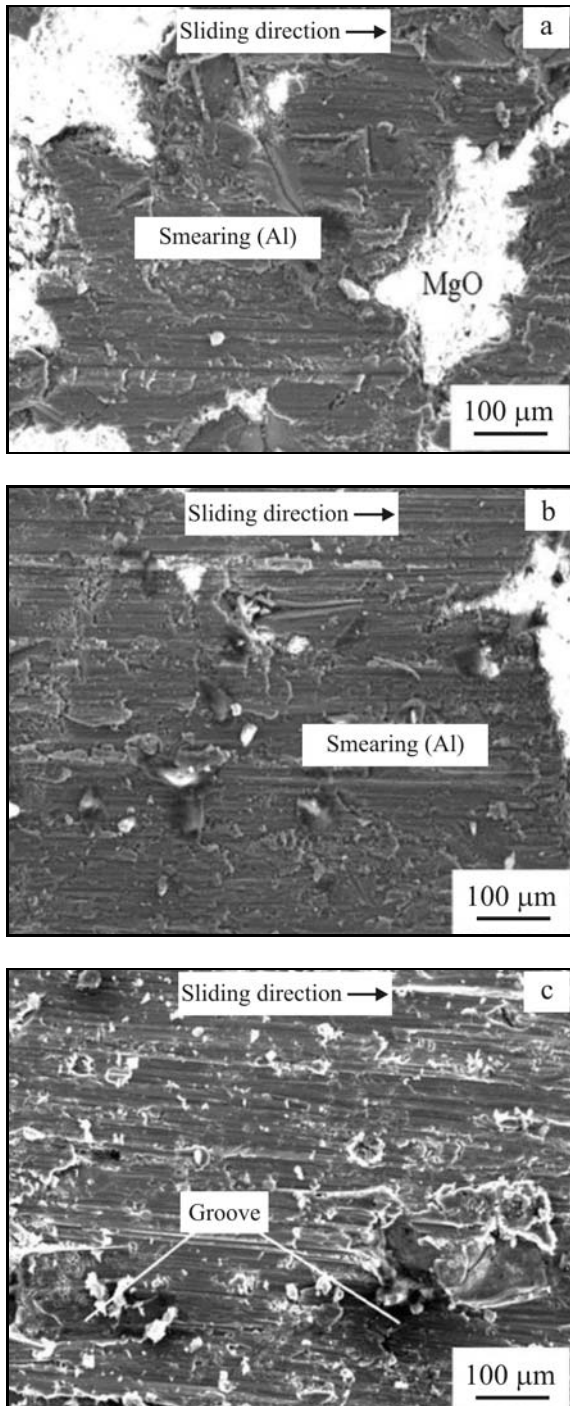


Fig. 11. SEM images of the worn surfaces of the Al-20%MgO composite tested at different loads: (a) 10 N, (b) 20 N and (c) 30 N at a sliding speed of  $1 \text{ m s}^{-1}$  for a sliding distance of 40 m.

ites increased continuously with increasing MgO content, Fig. 4. Continuous increase in the hardness of the composites with increasing MgO content can be related to the amount of relatively hard and brittle MgO particles in their microstructures. It is known that porosity has an adverse effect in hardness. How-

ever, it was observed that the porosity of the composites increased with increasing MgO content. It can be said that the volume fraction of hard and brittle MgO particles is more effective in hardness than porosity of the composites.

The tensile strength of the composites increased with increasing MgO content up to 20 %, above which the tensile strength decreased with increasing MgO content. Changes in tensile strengths of the composites may be explained in terms of distribution of the hard MgO particles and porosity of the composites. These particles in the composites showed more homogeneous distribution and resulted in a gradual increase in tensile strength, Figs. 3a–d. However, MgO particles showed a tendency to pile up in different locations in the composites containing more than 20 % MgO. It is known that the piling of hard particles in the composites results in a reduction in their strength by giving rise to cracking tendency [22–24]. On the other hand, the porosity of the composites increased above the 20 % MgO content. It is also known that the strength of the composites decreased with increasing porosity rate [10, 13]. Therefore, the reduction would be expected in tensile strength of the composites when their MgO content exceeded 20 %.

The wear volume of the composites decreased with increasing MgO content up to 20 %, above the trend reversed, Figs. 5–7. It is known that the wear volume of the composites is related to their tensile strength and porosity [25]. The volume loss of the composites decreases with increasing tensile strength. Porosity has an adverse effect on the volume loss of the samples. In view of the above, Al-20%MgO composite would be expected to exhibit the lowest wear volume. It was observed that the wear volume of the composites increased with increasing load and sliding speed, Figs. 8 and 9. The increase in the wear loss due to load is consistent with the Archard equation which states that the volume of wear material is proportional to the normal load or pressure between the contacting surfaces [26]. The increase in the wear loss due to sliding speed may be related to the production rate of the wear particles and centrifugal force acting on them. As the sliding speed increases the production rate of the wear particles would be expected to increase. As the centrifugal force increases the amount of loose particles scattered from the surface of the rotating disc is expected to increase. This may reduce the amount of smeared material on the surface of the wear samples and give rise to higher wear volume.

The wear surfaces of the composites were characterized by smearing, scratches and grooves, Fig. 10. Smearing may have resulted from the back transfer of the wear material from disc to sample surface, while the scratches are produced by ploughing action of the hard wear particles during either their removal or back transferring.

## 5. Conclusion

The porosity rate of the composites produced decreases with increasing volume ratio up to 20 % MgO, above this level the trend reversed. The hardness and tensile strength of the MMCs increased with increasing MgO content, but the trend reversed for the tensile strength higher than 20 % MgO. Although adhesion and abrasion took place during the wear of tested composites, smearing appeared to be the most effective wear mechanism for the composites containing up to 20 vol.% MgO, while abrasive wear dominated for the Al-30vol.%MgO and Al-40vol.%MgO composites. Wear resistance of the composites tested was observed to be strongly dependent on their tensile strength and porosity rather than their hardness. The Al-20vol.%MgO composite can be used for different tribological applications.

## Acknowledgements

Author would like to thank all technicians in the Materials Division of the Materials and Metallurgy Engineering Department of Kirikkale University for their help.

## References

- [1] Zhang, L. F., Zhang, L. C., Woo, Y. W.: J. Mater. Sci., 30, 1995, p. 5999. [doi:10.1007/BF01151519](https://doi.org/10.1007/BF01151519)
- [2] Deuis, R. L., Subramanian, C., Yellup, J. M.: Wear, 201, 1996, p. 132. [doi:10.1016/S0043-1648\(96\)07228-6](https://doi.org/10.1016/S0043-1648(96)07228-6)
- [3] Jiang, Q. C., Wang, H. Y., Zhao, Y. G., Li, X. L.: Mater. Res. Bull., 40, 2005, p. 521. [doi:10.1016/j.materresbull.2004.11.002](https://doi.org/10.1016/j.materresbull.2004.11.002)
- [4] Sawla, S., Das, S.: Wear, 257, 2004, p. 555. [doi:10.1016/j.wear.2004.02.001](https://doi.org/10.1016/j.wear.2004.02.001)
- [5] Uygur, I., Kulekci, M. K.: Turk. J. Eng. Environ. Sci., 26, 2002, p. 265.
- [6] Shen, Y. L., Williams, J. J., Piotrowski, G., Chawla, N., Guo, Y. L.: Acta. Mater., 49, 2001, p. 3219. [doi:10.1016/S1359-6454\(01\)00226-9](https://doi.org/10.1016/S1359-6454(01)00226-9)
- [7] Izciler, M., Muratoglu, M.: J. Mater. Process. Technol., 132, 2003, p. 67. [doi:10.1016/S0924-0136\(02\)00263-7](https://doi.org/10.1016/S0924-0136(02)00263-7)
- [8] Rabiei, A., Enoki, M., Kishi, T.: Mater. Sci. Eng. A, 293, 2000, p. 81. [doi:10.1016/S0921-5093\(00\)01218-1](https://doi.org/10.1016/S0921-5093(00)01218-1)
- [9] Xiuqing, Z., Haowei, W., Lihua, L., Xinying, T., Naiheng, M.: Mater. Lett., 59, 2005, p. 2105. [doi:10.1016/j.matlet.2005.02.020](https://doi.org/10.1016/j.matlet.2005.02.020)
- [10] Rabiei, A., Kim, B. N., Enoki, M., Kishi, T.: Mater. Trans. JIM, 37, 1996, p. 1148.
- [11] Isil, K., Toptan, F.: Mater. Lett., 62, 2008, p. 1215. [doi:10.1016/j.matlet.2007.08.015](https://doi.org/10.1016/j.matlet.2007.08.015)
- [12] Abejonar, J., Velasco, F., Martinez, M. A.: J. Mater. Process. Technol., 18, 2007, p. 441.
- [13] Guedes, M., Ferreira, J. M. F., Rocha, L. A., Ferro, A. C.: Ceram. Int., 37, 2011, p. 3631. [doi:10.1016/j.ceramint.2011.06.022](https://doi.org/10.1016/j.ceramint.2011.06.022)
- [14] Bai, L., Xitjuan, L., Mingjun, L., Zhenyu, Z.: Mater. Manuf. Process., 26, 2011, p. 1339. [doi:10.1080/10426914.2010.544813](https://doi.org/10.1080/10426914.2010.544813)
- [15] Qin, Q. D., Zhao, Y. G., Liu, C., Zhou, W., Ji-ang, Q. C.: Mater. Sci. Eng. A, 460, 2007, p. 604. [doi:10.1016/j.msea.2007.01.103](https://doi.org/10.1016/j.msea.2007.01.103)
- [16] Ramesh, C. S., Keshavamurthy, R., Channabasappa, B. H., Pramod, S.: Tribol. Int., 43, 2010, p. 623. [doi:10.1016/j.triboint.2009.09.011](https://doi.org/10.1016/j.triboint.2009.09.011)
- [17] Calin, R., Citak, R.: Mater. Sci. Forum, 546, 2007, p. 611. [doi:10.4028/www.scientific.net/MSF.546-549.611](https://doi.org/10.4028/www.scientific.net/MSF.546-549.611)
- [18] Gustafson, T. W., Panda, P. C., Song, G., Raj, R.: Acta. Mater., 45, 1997, p. 1633. [doi:10.1016/S1359-6454\(96\)00277-7](https://doi.org/10.1016/S1359-6454(96)00277-7)
- [19] Sreekumar, V. M., Pilla, R. M., Pai, B. C., Chakraborty, M.: J. Alloy. Compd., 461, 2008, p. 501. [doi:10.1016/j.jallcom.2007.07.032](https://doi.org/10.1016/j.jallcom.2007.07.032)
- [20] Nowak, R., Sobczak, N., Sienicki, E., Morgiel, J.: Solid State Phenom., 172–174, 2011, p. 1273. [doi:10.4028/www.scientific.net/SSP.172-174.1273](https://doi.org/10.4028/www.scientific.net/SSP.172-174.1273)
- [21] Calin, R.: Asian J. Chem., 22, 2010, p. 808.
- [22] Iwai, Y., Yoneda, H., Honda, T.: Wear, 181–183, 1995, p. 594.
- [23] Savaşkan, T., Alemdağ, Y.: Mater. Sci. Eng. A, 496, 2008, p. 517. [doi:10.1016/j.msea.2008.06.008](https://doi.org/10.1016/j.msea.2008.06.008)
- [24] Bican, O., Savaşkan, T.: Tribol. Lett., 37, 2010, p. 175. [doi:10.1007/s11249-009-9509-4](https://doi.org/10.1007/s11249-009-9509-4)
- [25] Avner, S. H.: Introduction to Physical Metallurgy. New York, McGraw Hill 1974.
- [26] Halling, J.: Principles of Tribology. Basingstoke, Macmillan Education Ltd. 1989.